RadioGraphics

Multidetector CT of Aortic Dissection: A Pictorial Review[1]

Michelle A. McMahon, FRCR • Christopher A. Squirrell, FRCR

ONLINE-ONLY CME

See www.rsna.org/education/rg_cme.html

LEARNING OBJECTIVES

After reading this article and taking the test, the reader will be able to:

- Identify the two types of aortic dissection and list the indications for treatment.
- Describe the imaging parameters and the typical and atypical imaging findings in aortic dissections.
- Discuss the imaging features of complications that can arise from aortic dissections.

TEACHING POINTS

See last page

Aortic dissection is the most common acute emergency condition of the aorta and often has a fatal outcome. Outcome is determined by the type and extent of dissection and the presence of associated complications (eg, cerebral sequelae, aortic branch involvement, pericardial involvement, and visceral involvement), with early diagnosis and treatment being essential for improved prognosis. Aortic dissections are classified on the basis of the site of the intimal tear according to the Stanford classification system. Type A aortic dissection involves the ascending thoracic aorta and may extend into the descending aorta, whereas in a type B dissection the intimal tear is located distal to the left subclavian artery. Type A dissection typically requires urgent surgical intervention, whereas type B dissection can often be treated medically. Modern multidetector computed tomography (CT) is a fast, widely available imaging modality with high sensitivity and specificity. Multidetector CT allows the early recognition and characterization of aortic dissection as well as determination of the presence of any associated complications, findings that are essential for optimizing treatment and improving clinical outcomes.

Introduction

Aortic dissection is the most common acute emergency condition of the aorta, often resulting in the death of the patient. A recent study identified rupture as the cause of death in approximately one-third of affected patients admitted to the hospital, although the rate of nonfatal rupture may be considerably higher (1,2). The incidence of aortic dissection has been reported to be 2,000 new cases per year in the United States and 3,000 in Europe (2–5). The overall outcome is determined by the type and extent of dissection and the presence of associated complications; therefore, evaluation of the entire aorta, branch vessels, and iliac and proximal femoral arteries is recommended to aid in treatment planning.

Abbreviations: ECG = electrocardiographic, TEE = transesophageal echocardiography

RadioGraphics 2010; 30:445–460 • **Published online** 10.1148/rg.302095104 • **Content Codes:** CA CT ER

[1]From the Department of Radiology, City Hospital Campus, Nottingham University Hospitals NHS Trust, Hucknall Rd, Nottingham, NG5 1PB, England (M.A.M.); and Department of Radiology, King's Mill Hospital, Nottingham, England (C.A.S.). Presented as an education exhibit at the 2008 RSNA Annual Meeting. Received April 27, 2009; revision requested June 30; final revision received December 12; accepted December 14. All authors have no financial relationships to disclose. **Address correspondence to** M.A.M. (e-mail:*mmcm75@yahoo.com*).

Early diagnosis and treatment are essential for improving the prognosis. Patients may present with the classic history of acute-onset tearing central chest pain that radiates to the back. Malperfusion symptoms may result from dissection-related side branch obstruction. It has been reported that up to 20% of patients with acute aortic dissection may present with syncope without a history of typical pain or neurologic findings (6–13). Syncope can result from hypotension secondary to cardiac tamponade (14,15) or from obstruction of cerebral vessels. Aortic regurgitation gives rise to a diastolic murmur, which has been reported in 40%–50% of patients with proximal dissections (3), and severe regurgitation can result in heart failure (12,14,15). Cerebrovascular manifestations and limb ischemia with pulse deficits may occur due to side branch orifice involvement by the dissection flap or obliteration of the true lumen by an expanding false lumen (2,16). Abdominal pain can be an indicator of abdominal branch involvement, whereas oliguria and anuria are indicators of renal artery involvement. Compression of adjacent structures such as the superior vena cava, left laryngeal nerve, bronchi, and esophagus can give rise to corresponding signs and symptoms.

In this article, we discuss and illustrate aortic dissection in terms of definition and pathophysiologic features, types of dissection, radiologic options, imaging parameters, imaging features, multidetector computed tomographic (CT) pitfalls, and associated complications.

Definition and Pathophysiologic Features of Aortic Dissection

Teaching Point

Dissection is the result of a spontaneous longitudinal separation of the aortic intima and adventitia caused by circulating blood gaining access to and splitting the media of the aortic wall (17). The intimal tear allows blood to enter the media from the vessel lumen. The blood-filled space within the medial layer becomes the false lumen. This results in two lumina— a true lumen and a false lumen—with the false lumen having pressures greater than or equal to those in the true lumen (18). In an in vitro study, Williams et al (19) postulated that the true lumen collapses due to loss of transmural pressure across the dissection flap, which has become detached from its connective tissue attachment, thereby reducing the elastic recoil and shortening the flap. The elastic flap is released from transmural pressure, and it contracts and does not respond to absolute aortic pressures. There is expansion of the false lumen due to reduced elastic recoil in its thin outer wall, which contains only about one-third of the baseline elastin. The elastin-poor outer wall of the false lumen then dilates more than the elastin-rich nondissected baseline wall to generate the wall tension required to balance a given blood pressure. Ultimately, the tension in the thin outer wall may become so great as to cause rupture of the false lumen. The overall degree of dilatation depends on the blood pressure, residual wall thickness (depth of dissection plane in the media), and percentage of the wall circumference involved in the dissection (19). The dissection may move in either an antegrade or retrograde direction. Because of pressure differences, the false lumen may compress or obstruct the true lumen. In general, the dissection may remain patent as a false lumen, thrombose, recommunicate with the true lumen through fenestrations, or rupture into potential spaces such as the pericardial, pleural, or peritoneal cavities (20). The type of dissection is determined by the site of origin of the intimal tear (Fig 1). Arteries supplied exclusively by the false lumen are rarely compromised (18).

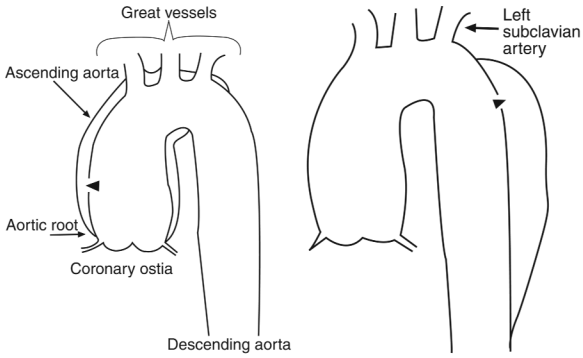

Figure 1. **(a)** Drawing (sagittal view) illustrates type A aortic dissection. The intimal flap (arrowhead) arises from the ascending aorta and may extend into the descending aorta. **(b)** Drawing (sagittal view) illustrates type B aortic dissection. The dissection flap (arrowhead) arises from the descending aorta distal to the left subclavian artery.

Two types of branch-vessel obstruction are described in the literature: static and dynamic obstruction. With static obstruction, the intimal flap enters the branch-vessel origin (1) without a reentry point (21). This results in increased pressure or thrombus formation in the false lumen within the branch vessel, causing focal stenosis and end-organ ischemia (21). Static obstruction is treated with intravascular stent placement (18,22). Dynamic obstruction affects vessels arising from the true lumen. The intimal flap spares the branch vessel but prolapses and covers the branch-vessel origin like a curtain, causing a pressure deficit in the true lumen that results in

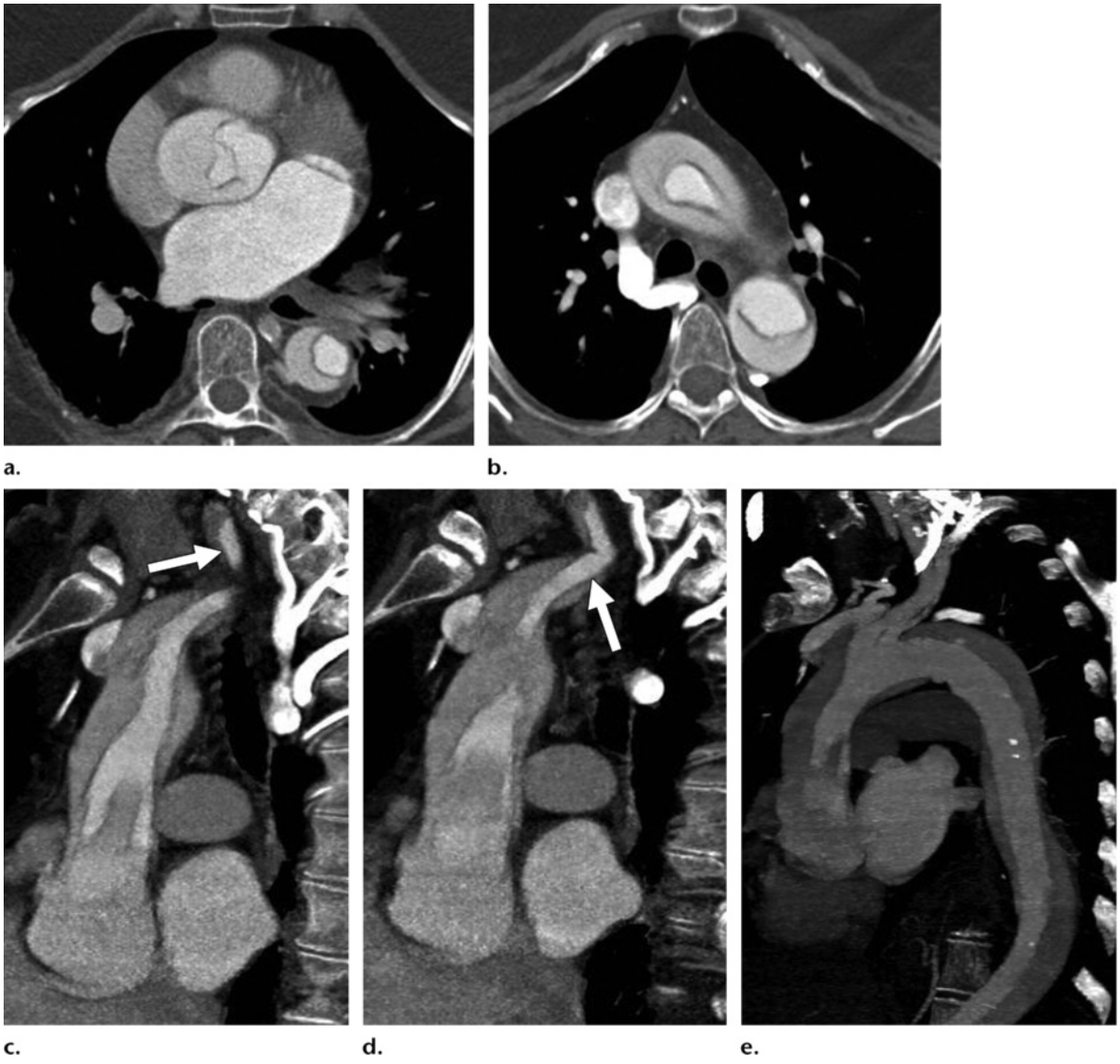

Figure 2. **(a, b)** Stanford type A aortic dissection. **(a)** Axial image through the thorax shows dissection flap involvement of the aortic root and descending aorta. **(b)** Axial image through the thorax shows the dissection flap in the aortic arch. **(c–e)** Type A aortic dissection in a different patient. **(c, d)** Sagittal reformatted images through the thorax and upper abdomen obtained at different levels from 64-section multidetector CT show intimal flap involvement of the ascending thoracic aorta. Note the extension of the dissection flap into aortic branch vessels (arrow). **(e)** Sagittal maximum intensity projection image shows dissection flap involvement of both the ascending and descending aorta.

ischemia (1). Dynamic obstruction is treated with fenestration of the intimal flap to decrease the pressure in the false lumen (18,22).

By definition, acute aortic dissections are characterized by symptoms that are present for less than 14 days; in chronic dissections, the symptoms are present for a longer period (23).

Definition of Types of Dissection

The Stanford classification system for dissections is based on the need for surgical intervention (24).

Teaching Point

Stanford type A dissection involves the ascending thoracic aorta, and the dissection flap may extend into the descending aorta. Type A dissections account for 60%–70% of cases (17) and typically require urgent surgical intervention to prevent extension into the aortic root, pericardium, or coronary arteries (1). If untreated, type A dissections are associated with a mortality rate of over 50% within 48 hours (Figs 1a, 2) (25).

Teaching Point

Stanford type B dissection involves the descending thoracic aorta distal to the left subclavian artery and accounts for 30%–40% of cases (Figs 1b, 3) (17). Management takes the form of medical treatment of hypertension, unless there are complications due to extension of the dissection (eg, end-organ ischemia or persistent pain) that would necessitate surgical intervention.

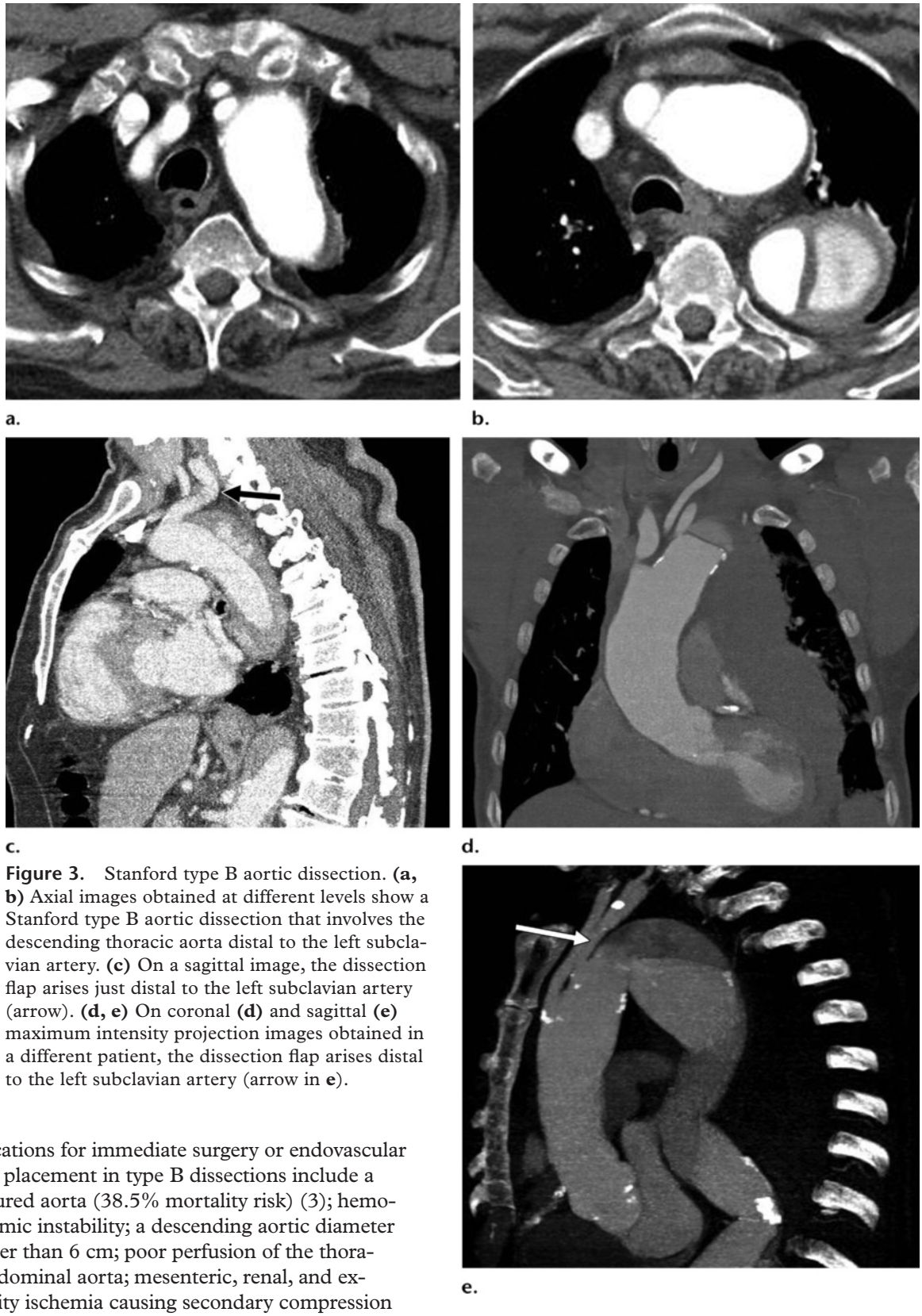

Figure 3. Stanford type B aortic dissection. **(a, b)** Axial images obtained at different levels show a Stanford type B aortic dissection that involves the descending thoracic aorta distal to the left subclavian artery. **(c)** On a sagittal image, the dissection flap arises just distal to the left subclavian artery (arrow). **(d, e)** On coronal **(d)** and sagittal **(e)** maximum intensity projection images obtained in a different patient, the dissection flap arises distal to the left subclavian artery (arrow in **e**).

Indications for immediate surgery or endovascular stent placement in type B dissections include a ruptured aorta (38.5% mortality risk) (3); hemodynamic instability; a descending aortic diameter greater than 6 cm; poor perfusion of the thoracoabdominal aorta; mesenteric, renal, and extremity ischemia causing secondary compression of the true lumen by the expanding false lumen (11); pseudocoarctation syndrome with uncontrolled hypertension (26); and distal embolization (27). Outcomes have been shown to be worse in patients with secondary retrograde involvement of the aortic arch and ascending aorta (26).

According to aortographic studies, in a type A aortic dissection, the dissection flap usually begins close to the aortic root and tends to lie anterolat-

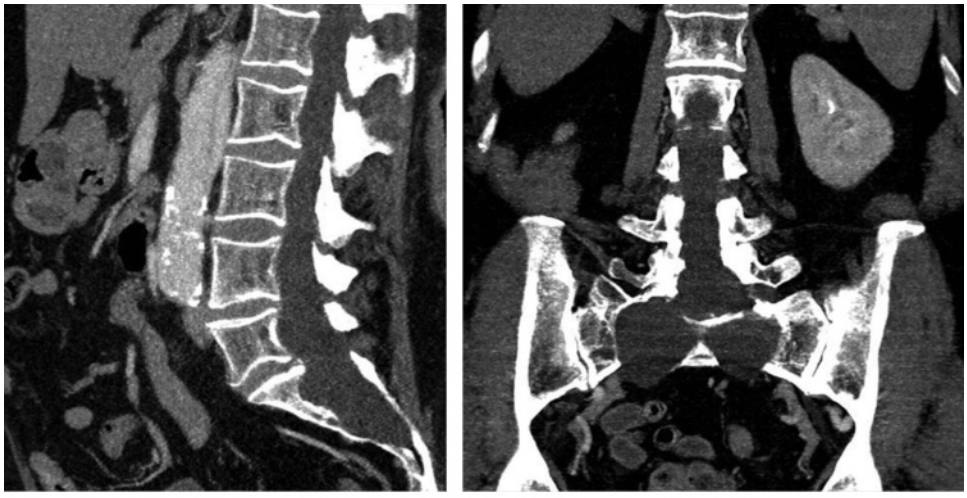

a. b.

Figure 4. Stanford type A aortic dissection that also involves the descending aorta in a patient with Marfan syndrome. Sagittal **(a)** and coronal **(b)** images of the lumbosacral spine show associated marfanoid features of dural ectasia and posterior scalloping of the lower lumbar vertebral bodies and sacrum, along with enlargement of the spinal canal.

eral to and to the right of the ascending aorta. If the dissection flap continues into the aortic arch, it tends to lie posterosuperiorly along the convexity. In the descending thoracic aorta, it tends to lie posterolateral to and to the left of the true channel down to the diaphragm. Below the diaphragm, it can spiral either anteriorly to involve the mesenteric vessels or posteriorly (28–31).

The most common risk factor for the development of an aortic dissection is hypertension, which occurs in 60%–90% of cases (3,17). Cystic medial necrosis and disease of the aortic wall also predispose to dissection. In an article by Hagan et al (3), Marfan syndrome was reported in 4.9% of patients with aortic dissection in the International Registry of Acute Aortic Dissection; therefore, it is important to look for associated features of possible underlying disease (Fig 4). Hagan et al (3) also reported a known history of aortic aneurysm in 12.4% of patients with type A aortic dissection and in 2.2% of patients with type B aortic dissection, with atherosclerosis of the aorta noted in 24.4% of type A aortic dissections and 42% of type B aortic dissections.

Rarer associations include other connective tissue diseases such as Ehlers-Danlos syndrome, relapsing polychondritis, Behçet disease, Turner syndrome, aortitis (systemic lupus erythematosus), and infections (14,32). Aortic root anomalies such as valvular aortic stenosis, coarctation, or bicuspid aortic valves also predispose to the development of dissections. Mechanical causes (eg, prosthetic valves, blunt trauma, or catheterization) are rare (17). Drugs such as cocaine have been documented as causative agents in patients without a known history of hypertension (33).

Radiologic Options

Chest radiographic findings may be normal in 10%–40% of aortic dissections. In the study by Hagan et al (3), a widened mediastinum was noted in 61.1% of aortic dissection cases. Displacement of calcification of the aorta was reported in 14.1% of cases, with an abnormal cardiac contour being noted in 25.8% (3). Marked enlargement of the heart indicating a pericardial effusion or the presence of a new pleural effusion is suggestive of complications from aortic dissection.

Electrocardiographic (ECG) findings may be normal unless there has been compromise of the coronary arteries giving rise to an acute coronary syndrome with associated findings on the ECG tracing. No specific biochemical markers are available for detection of an aortic dissection.

Transthoracic echocardiography is a noninvasive examination that may help detect an ascending aortic dissection flap. It has a reported sensitivity of 59%–83% and a specificity of 63%–93% for the diagnosis of aortic dissection. The sensitivity of transthoracic echocardiography is between 78% and 100% for the diagnosis of a type A dissection, but it is only 31%–55% for dissections involving the descending aorta (24,34–36). Transesophageal echocardiography (TEE) is reported to have a sensitivity of 94%–100% and a specificity of 77%–100% for identifying an intimal flap (37,38). However, the distal part of the ascending aorta and the branches of the aortic arch may not be adequately evaluated with TEE (39). One possible problem with TEE is the potential "blind spot" due to the position of the trachea between the

esophagus and the upper ascending aorta (36,40). In patients with an identifiable dissection flap, secondary signs of an aortic dissection such as aortic root dilatation, aortic regurgitation, coronary ostial patency, pericardial effusions, or regional abnormal wall motion can be diagnosed (36). TEE can be performed in the emergency department at the bedside of unstable patients, thereby helping prevent delays in accurate diagnosis and treatment. At many centers, however, the value of TEE is limited by a lack of availability and expertise.

At CT, ECG gating allows more precise delineation of the proximal extent of the mural flap in relation to the aortic valve and coronary arteries and, more importantly, helps avoid overdiagnosis of aortic dissections caused by misinterpretation of a motion artifact as a mural flap. In practice, cardiac gating is becoming standard procedure for CT angiography of suspected aortic dissections. In patients with a previously diagnosed type B aortic dissection, follow-up studies can be performed in a nongated mode, since delineation of disease in the distal aortic arch and descending thoracic aorta does not require cardiac gating.

Contrast material–enhanced magnetic resonance (MR) angiography is more suitable for the investigation of aortic dissection in medically stable patients or those with chronic dissections. This modality is accurate and noninvasive, has excellent spatial and contrast resolution, and allows multivascular imaging phases with fast postprocessing (41–43). Three-dimensional contrast-enhanced MR angiography can *(a)* provide a complete and dynamic display of aortic dissection; *(b)* help determine the type of dissection; and *(c)* display the true and false lumina, the intimal flap, the location and size of the initial entry and its relationship with the neighboring arterial orifice, the origin of the aortic branches, and the presence and amount of thrombus in the false lumen, which is important for planning of surgical and endovascular therapy as well as for proper pre-and postoperative assessment and follow-up (41–43). Contrast-enhanced MR angiography has several advantages over CT angiography, including lack of nonionizing radiation, multiplanar evaluation, and greater vessel coverage at high resolution with fewer sections. In addition, postprocessing is much faster with contrast-enhanced MR angiography than with CT angiography (42,44–46), and contrast-enhanced MR angiography does not require the removal of bone structures for adequate visualization of the vasculature (41–43).

Nevertheless, three-dimensional contrast-enhanced MR angiography has its limitations. It cannot be performed in unstable patients due to longer acquisition time and difficulty in monitoring, and it is not appropriate for patients with implanted electronic devices. Moreover, the accuracy of display is operator dependent, and calcification of the arterial wall or intimal flap cannot be visualized. In addition, contrast-enhanced MR angiography may be of limited value in follow-up studies performed after endovascular treatment because of artifacts related to the metallic composition of the stent (44,47).

CT, including helical CT and multisection CT, has the advantages of shorter acquisition time, wide availability, and high diagnostic accuracy and has, therefore, classically been the modality of choice for the evaluation of aortic dissection.

Triple-rule-out CT is a new protocol used to assess the aorta, coronary arteries, and pulmonary arteries and the middle and lower portions of the lungs during a single scan with use of several optimally timed boluses of contrast material and ECG gating in patients who are at low risk for acute coronary syndrome. The aim is to minimize the contrast material dose and radiation exposure while achieving optimal image quality, providing coronary artery image quality equivalent to that of dedicated coronary CT angiography, pulmonary artery image quality equivalent to that of dedicated pulmonary CT arteriography, and high-quality images of the thoracic aorta without pulsation artifact. Optimal image quality is achieved with use of ECG gating. Although a regular cardiac rhythm remains an important factor in coronary CT image quality, newer CT scanners with 64 or more detectors allow rapid ECG-gated imaging, thereby providing high-quality triple-rule-out CT studies in patients with a heart rate of up to 80 bpm (48). Biphasic injection of iodinated contrast material (≤100 mL) is tailored to provide simultaneous high levels of arterial enhancement in the coronary arteries and aorta (>300 HU) and in the pulmonary arteries (>200 HU) (48). Scanning parameters, including prospective ECG tube current modulation and prospective ECG gating, are tailored to reduce radiation exposure (optimally, 5–9 mSv) (48). In an appropriately selected emergency department patient population, triple-rule-out CT can safely eliminate the need for further diagnostic testing in over 75% of patients (48).

Modern multisection CT allows rapid image acquisition and data reconstruction and aids in treatment planning. It helps differentiate type A from type B dissection, may localize the intimal entry site, and helps assess branch-vessel in-

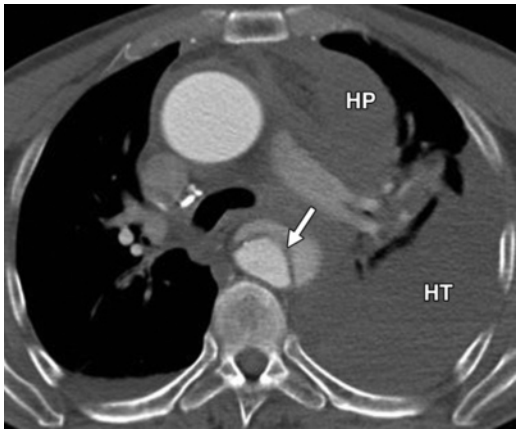

Figure 5. Intimal flap. Axial image through the thorax shows an intimal dissection flap in the descending aorta (arrow). Secondary findings of mediastinal hematoma, hemothorax *(HT)*, and hemopericardium *(HP)* are also depicted.

volvement and compromise and the relationship of the branch vessels to the true or false lumen. This information aids in planning treatment with either root replacement, intravascular stent placement, or fenestration.

In a comprehensive meta-analysis of MR imaging, TEE, and helical CT findings, patients with a 50% pretest probability of thoracic aortic dissection (high risk) had a 96%, 93%, and 93% posttest probability of thoracic aortic dissection following a positive result at these three modalities, respectively (37). In contrast, patients with a 5% pretest probability of thoracic aortic dissection (low risk) had a 0.3%, 0.2%, and 0.1% posttest probability of thoracic aortic dissection following a negative result at MR imaging, TEE, and helical CT, respectively (37). Helical CT yielded a sensitivity of 100% and a specificity of 98%, and it was superior to the other two modalities in ruling out thoracic aortic dissection in patients at low risk for thoracic aortic dissection (37).

Imaging Parameters

Images are obtained with a 64-detector CT scanner, with coverage from the lung apices to the groin. Automatic triggering is set at 110 HU. A 100-mL bolus of nonionic contrast material with a saline chaser is injected at a rate of 3–4 mL/sec via a 20-gauge (or larger) intravenous cannula. Section thickness is 1 mm.

ECG gating allows delineation of the aortic root and of coronary artery involvement. It also allows clear differentiation of motion artifact in the ascending aorta from true aortic dissection.

ECG gating techniques are used to minimize imaging artifacts caused by cardiac motion. Two methods are used: prospective ECG triggering and retrospective ECG gating. In cardiac diastole, the ventricles fill passively, resulting in reduced cardiac motion. Prospective ECG triggering uses the ECG signal to control scanning so that x-rays are generated and projection data are acquired during diastole only (49). With multidetector CT, the entire scan can be performed during a single breath hold. The start of diastole is estimated from the previous three to seven consecutive heartbeats and occurs about 450 msec prior to the R wave on the ECG tracing. Limitations of the prospective method are sensitivity to heartbeat variations (the examination is more effective at a heart rate of <90 bpm) and arrhythmias (49).

The radiation exposure in retrospectively ECG-gated CT angiography is higher than that in nongated chest protocols (50). In retrospective ECG gating, partially overlapping multidetector CT projections are continuously acquired with the ECG signal simultaneously recorded. Specific algorithms are then used to organize data from selected phases of the cardiac cycle to generate the resultant image (49).

Factors that are important in reducing the radiation dose include patient positioning in the center of the scanning field, heart rate control, pitch, and collimation. Radiation dose should be high enough to maintain an appropriate contrast-to-noise ratio for diagnostic-quality images, but no higher (49).

Roos et al (50) quoted doses of 3.65, 8.85, and 4.50 mSv for prospectively triggered, retrospectively gated, and nongated CT angiography of the aorta, respectively, covering a range of 15 cm. Equivalent doses of 5–7 mSv for retrospectively gated CT angiographic examinations of the coronary arteries have been described (51), whereas conventional angiography requires an average dose of approximately 5 mSv (52).

Imaging Features of Aortic Dissection

Teaching Point

The classic intimal flap is seen in approximately 70% of cases of aortic dissection. It occurs when blood enters the medial layer through an intimal tear, giving rise to a true lumen and a false lumen, with the flap separating the two lumina (Fig 5) (53).

A circumferential intimal flap occurs due to dissection of the entire intima (53). A narrow true lumen with a filiform shape may be seen and an intimointimal intussusception can subsequently occur, giving rise to a "windsock" appearance (Fig 6) (54,55).

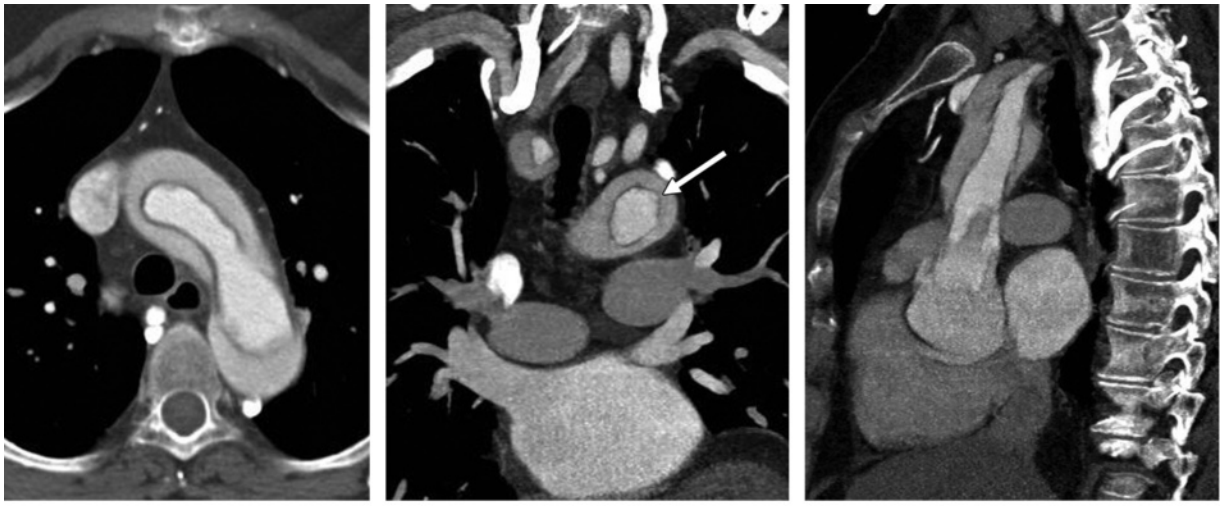

a. b. c.

Figure 6. Atypical appearances of an aortic dissection. Axial **(a)**, coronal **(b)**, and sagittal **(c)** images show atypical appearances of an aortic dissection, including circumferential dissection of the intimal layer (arrow in **b**). Intimointimal intussusception can subsequently occur, giving rise to a windsock appearance. The intima usually tears near the coronary orifices. The inner lumen is usually the true lumen.

Figure 7. Mercedes-Benz sign. Axial image through the thorax shows a three-channel dissection of the descending aorta due to a secondary dissection within one of the channels. (Reprinted, with permission, from reference 49.)

Figure 8. Cobweb sign in a patient with aortic dissection. Axial image shows wispy structures that are similar in attenuation to the dissection flap within the false lumen. These structures are thought to represent strands of media that separate incompletely during the dissection process (arrow), and they are thought to be specific for the false lumen.

A calcified false lumen can be seen in chronic dissections with mural calcification of the false lumen (56). Rarely, a three-channel dissection can be seen if a secondary dissection occurs within one of the channels, with the resultant intimal flaps giving rise to the "Mercedes-Benz sign" (Fig 7) (29,57).

Differentiation of the true lumen from the false lumen is important for planning endovascular interventional procedures. Important signs that indicate the false lumen include a larger cross-sectional area, the "cobweb sign," and the "beak sign." Williams et al (58) described the cobweb sign as slender linear areas of low attenuation specific to the false lumen due to residual ribbons of media that have incompletely sheared

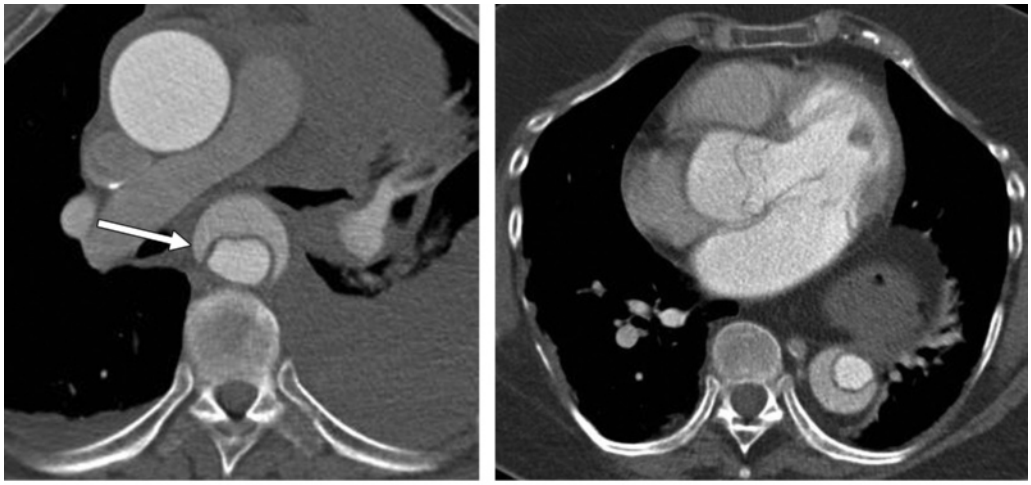

a. b.

Figure 9. Beak sign. **(a)** Axial image demonstrates the beak sign (arrow). A wedge of hematoma is thought to create a space for the development of the false lumen. In this case, the dissection is complicated by a pericardial, mediastinal, and pleural hematoma. **(b)** Axial image obtained in a different patient again shows the beak sign, which is seen in the descending thoracic aorta. The site of the dissection is noted in the ascending aorta just distal to the aortic root. A hiatal hernia is incidentally noted.

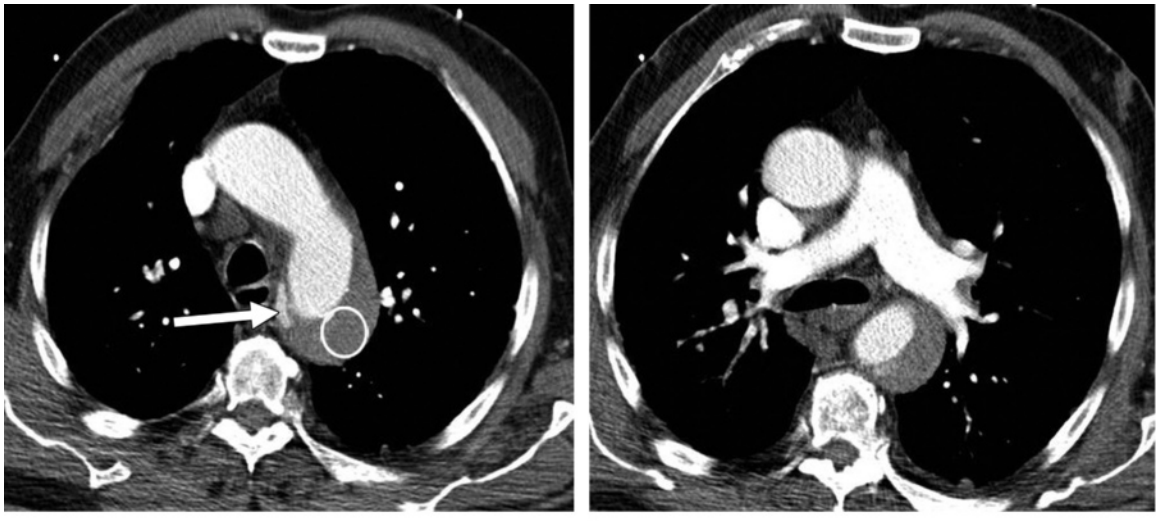

a. b.

Figure 10. Stanford type B aortic dissection. Contrast-enhanced CT scans obtained at different levels show a thrombosed false lumen (circle in **a**). Arrow in **a** indicates a small residual flow channel in the false lumen.

away during the dissection process (Fig 8). Le Page et al (59) described the beak sign seen at cross-sectional imaging as a wedge of hematoma that creates a space for the propagation of the false lumen (Fig 9). At contrast-enhanced CT, the true lumen is in continuity with the undissected portion of the aorta (1), and the false lumen may become thrombosed (Fig 10).

Secondary findings of aortic dissections include internal displacement of intimal calcification, delayed enhancement of the false lumen, widening of the aorta and mediastinum, and pleural or pericardial hematoma (60).

Although the aforementioned features can all be appreciated at contrast-enhanced CT of the aorta, it should be standard practice to perform a precontrast scan to assess for high attenuation within the aortic wall resulting from either a high-attenuation false lumen or the presence of intramural hematoma.

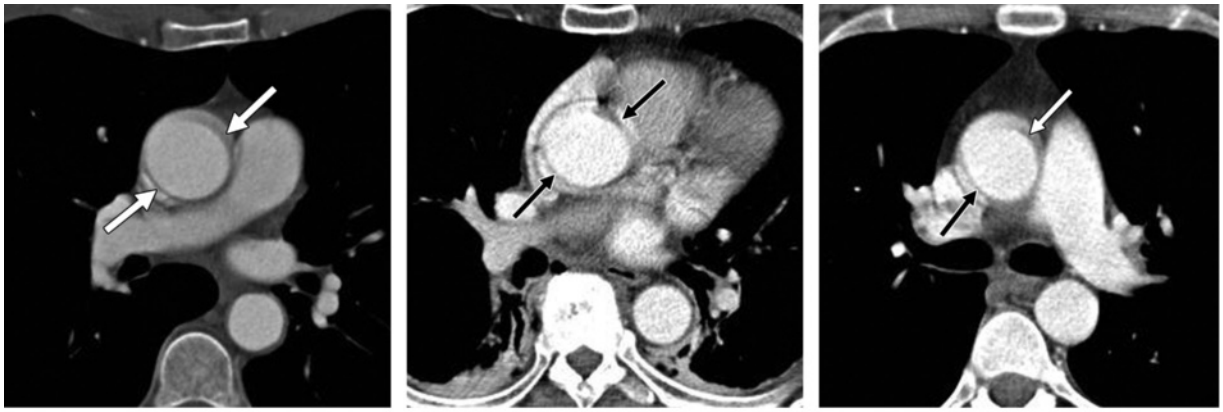

a. b. c.

Figure 11. Aortic motion artifact. Axial images through the thorax obtained at the level of the right pulmonary artery **(a)**, aortic root **(b)**, and main pulmonary artery **(c)** show aortic motion artifact (arrows) mimicking a dissection flap in the ascending aorta.

Pitfalls of Multidetector CT

Most of the artifacts at CT can be due to either *(a)* perivenous streaks from a combination of beam-hardening and motion artifacts from pulsations in veins carrying undiluted contrast material to the heart, or *(b)* aortic motion artifact (Fig 11) (61); such artifacts can lead to false-positive study results. The scanning rotation times for 64- and 16-detector CT are comparable, and their temporal resolutions are equivalent. The advantage of 64-detector CT is that fewer artifacts are recorded in the image because the volume acquisition is faster. However, misdiagnosis of aortic dissection secondary to motion artifact simulating an intimal flap in the ascending aorta still occurs at nongated 64-detector CT.

Multidetector CT has increased spatial and temporal resolution, resulting in faster, more versatile scanning with isotropic spatial resolution (62,63). Increased volume coverage increases speed and allows assessment of the aorta, pulmonary arteries, and coronary arteries during a single breath hold with a single continuous acquisition.

False-negative study results can occur due to inadequate contrast opacification caused by cardiac failure (17), or to the thrombosed lumen being mistaken for an aortic aneurysm with mural thrombus.

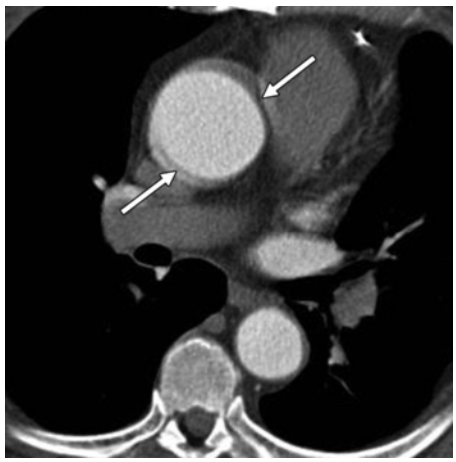

Figure 12. Pericardial recess. Axial image shows a pericardial recess (arrows) mimicking a dissection flap in the ascending aorta.

A number of findings can mimic an aortic dissection flap (53,64), and it is important to be aware of these mimics in practice. These findings include the pericardial recess (Fig 12) and a mural thrombus in a fusiform aneurysm. Periaortic fibrosis or mediastinal, pulmonary, or retroperitoneal tumors can also be mistaken for dissection flaps, as can anemia with apparent high attenuation of the aortic wall. Vascular structures around the aorta such as the aortic sinus, left brachiocephalic vein, and left superior intercostal vein (64) can also be mistaken for a dissection flap. Awareness of these mimics is important for preventing a false-positive diagnosis.

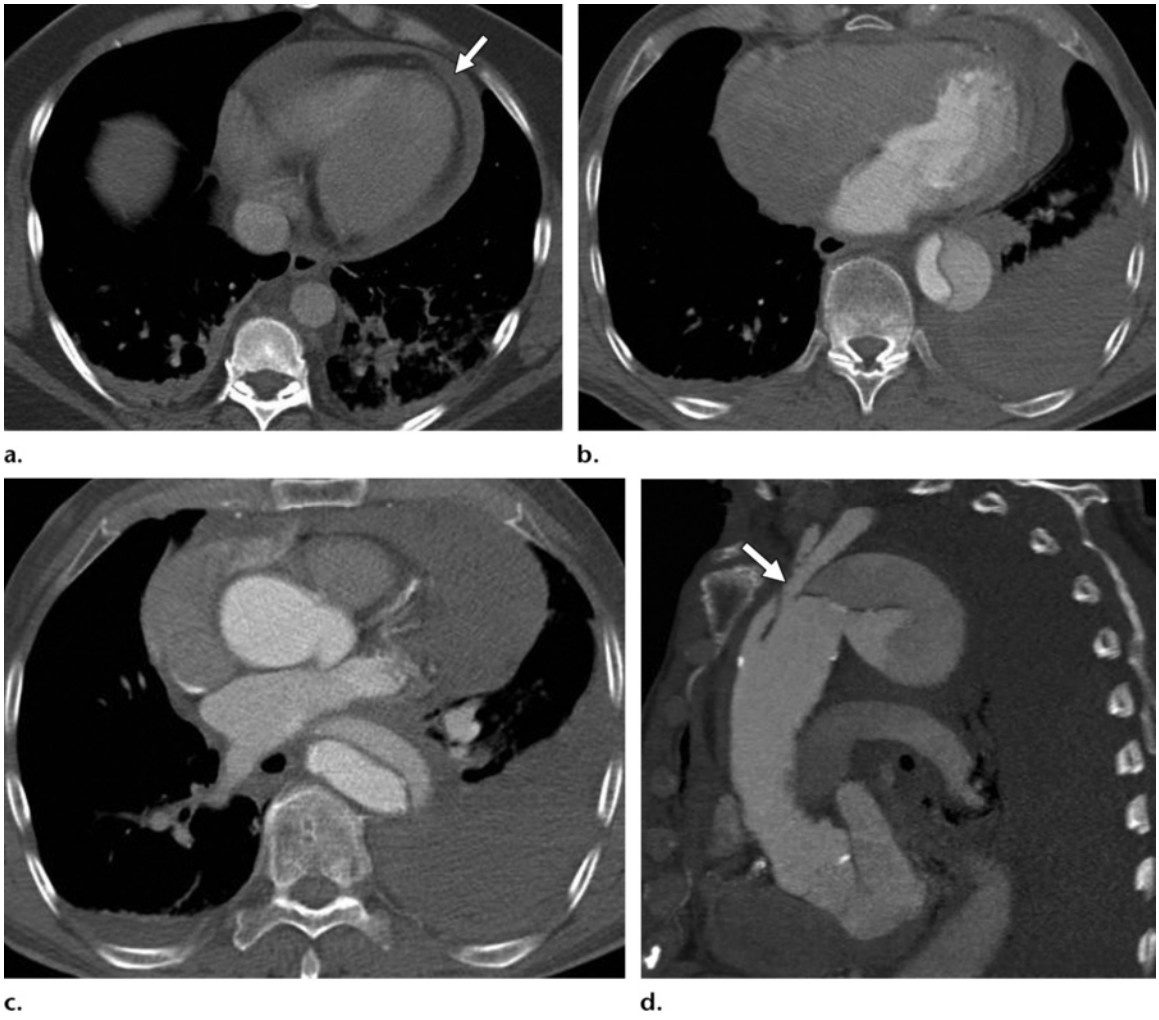

Figure 13. Stanford type A aortic dissection. **(a)** Axial image through the thorax shows a high-attenuation pericardial effusion (arrow) in keeping with a hemopericardium. **(b, c)** Axial images through the thorax obtained in a different patient show a high-attenuation pericardial effusion in keeping with a hemopericardium, as well as a left-sided pleural effusion–hemothorax. The dissection flap is clearly visible in the descending thoracic aorta. **(d)** Sagittal maximum intensity projection image shows the dissection flap distal to the left subclavian artery (arrow), along with hemopericardium and hemothorax.

Complications of Thoracic Aortic Dissection

Teaching Point

In patients with thoracic aortic dissection, death can occur secondary to acute aortic regurgitation, major aortic branch obstruction, pericardial tamponade, or aortic rupture, 75% of which occur into the pericardium, left pleural cavity, or mediastinum (Fig 13) (1). Rupture can also occur into the right ventricle, left atrium, vena cavae, or pulmonary arteries, producing a large left-to-right shunt (17). Imaging features of aortic rupture at unenhanced CT include a hyperattenuating mediastinal, pericardial, or pleural fluid collection. Contrast-enhanced CT demonstrates irregularity of the aortic wall and may depict extravasation of vascular contrast material (1).

Previous studies have shown that 33% of patients have signs or symptoms of other organ involvement (1).

Neurologic involvement occurs in up to 5%–10% of patients (1). This can include involvement of one or more branch vessels. It is important to

Figure 14. Brachiocephalic artery dissection. **(a)** Axial image through the superior mediastinum demonstrates a dissection flap in the right brachiocephalic artery (arrow). **(b)** Coronal image shows that the innominate artery receives blood from both the true and false lumina, whereas the left common carotid and subclavian arteries receive blood predominantly from the true lumen.

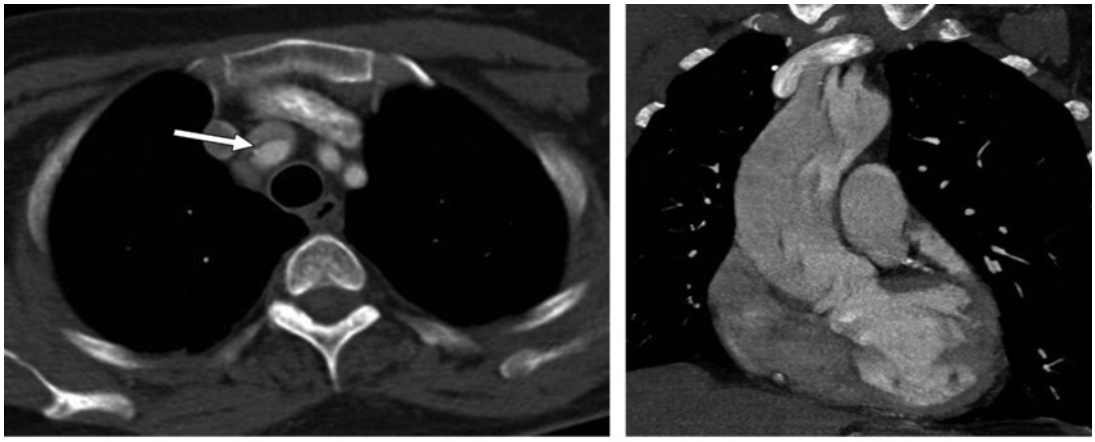

a. b.

include the main arterial branch vessels in the scanning range to ensure early diagnosis and aid in surgical planning to improve prognosis (Fig 14).

Main abdominal arterial branch involvement has been reported in 27% of cases (27), and the celiac trunk, superior and inferior mesenteric arteries, and renal arteries can all be involved. Occlusion of the celiac trunk may lead to splenic or hepatic infarction with pain and abnormal liver blood test results. Involvement of the mesenteric branches can lead to mesenteric ischemia with nausea, vomiting, nasogastric aspirates, abdominal pain, bloody diarrhea, recurrent sepsis, and abnormal hepatic and pancreatic enzymes (1).

Compromise of the renal arteries can lead to ischemia with oliguria, anuria, and abnormal renal blood parameters. Renal arteries supplied by the false lumen are rarely compromised (1).

Figure 15 illustrates a dissection flap near the origin of an abdominal branch vessel that could progress to either static or dynamic obstruction of the involved vessel. It is important to look at end organs such as the kidneys for evidence of involvement (eg, infarction or ischemia) (Figs 16–18) (1).

CT with 64 detectors has the spatial resolution needed to identify the coronary arteries. ECG gating is becoming the standard of care because it allows delineation of the aortic root and visualization of dissection flap involvement of the coronary arteries. Involvement of the coronary arteries requires urgent cardiothoracic surgery and is often fatal.

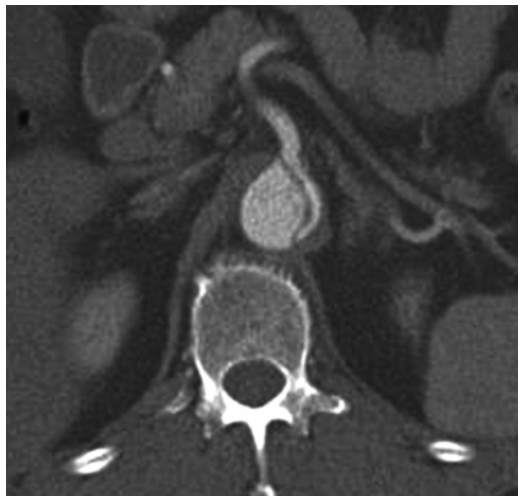

Figure 15. Dissection flap near the origin of the superior mesenteric artery. On an axial image, a dissection flap crosses the origin of the superior mesenteric artery. If the false lumen were to expand further, the dissection flap would progressively prolapse across the origin of the artery, causing dynamic obstruction of the vessel.

Extension of the dissection flap into the common femoral arteries may cause signs and symptoms of lower limb ischemia, with pain, cold peripheries, discoloration, pulse deficits, and gangrene. Therefore, it is recommended that the entire aorta and pelvic vessels down to the groin be included in the scanning field to detect the full extent of involvement (Fig 19) (1). Extension of a type B dissection into the iliac or femoral arteries has implications for management and procedure planning, especially when stent-graft placement is being considered. With respect to iliac and

Figures 16–18. Complications of thoracic aortic dissection. **(16)** Axial image through the abdomen shows dissection flap involvement of the origin of the superior mesenteric artery (arrow). The dissection flap is seen to enter the origin of the artery, thereby compromising its lumen. This type of obstruction is treated with intravascular stent placement. **(17a)** On an axial image through the abdomen obtained in a different patient, an unopacified false lumen flap extends into the left renal artery, and there is no contrast enhancement of the left kidney, a finding that is in keeping with profound ischemia-infarction. The right kidney is supplied by the true lumen and demonstrates normal enhancement. In contradistinction, in dynamic obstruction, the intimal flap prolapses across the renal artery origin, acting like a curtain and covering the renal ostium. **(17b)** Coronal image through the abdomen shows an unenhanced left kidney (arrow) in keeping with renal infarction-ischemia. The dissection flap is seen in the descending thoracic aorta. **(18)** Coronal image through the abdomen obtained in a third patient shows a clearly delineated area of low attenuation (hypoperfusion) in the left kidney (arrow), a finding that is consistent with acute renal infarction. The dissection flap is noted in the descending aorta.

16.

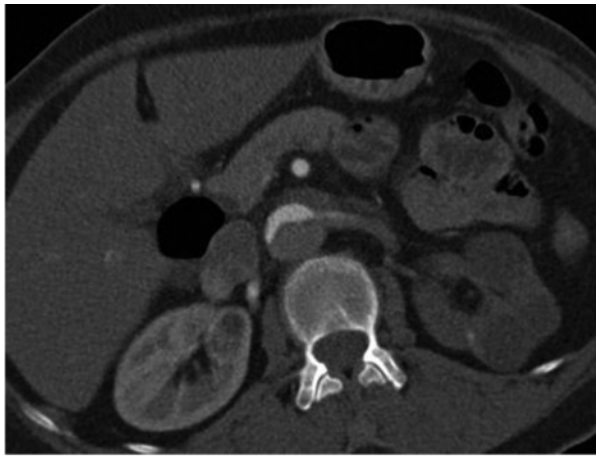

17a.

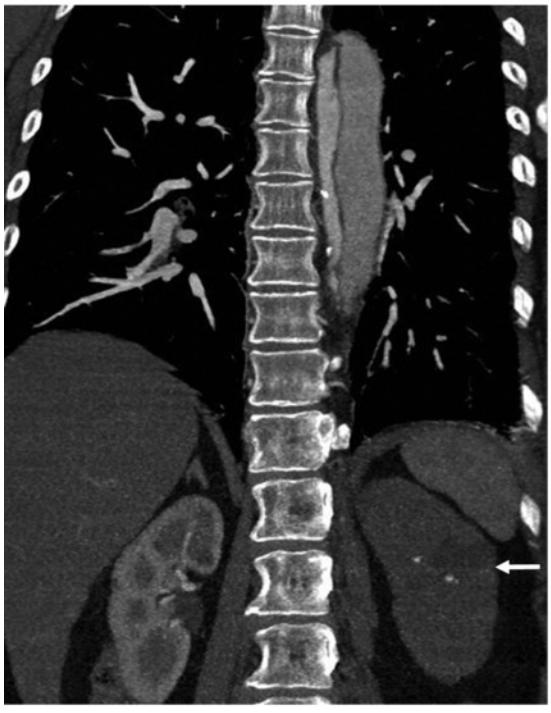

17b.

18.

femoral artery involvement, if a percutaneous intervention is being considered, it is important to determine whether the true lumen can be entered with a right or left femoral artery approach.

Conclusions

Aortic dissection is the most common acute emergency condition of the aorta and often leads to the patient's death. Early diagnosis and treatment are essential for improving the prognosis. It is recommended that the scanning field include the entire aorta and pelvic vessels to help determine the type and extent of dissection and to help detect complications early enough to improve outcome and aid in treatment planning.

CT imaging of the aorta is fast and widely available, which are important features in making an accurate diagnosis quickly in unstable patients. Multidetector CT allows imaging of the entire aorta with rapid acquisition and data reconstruction to provide prompt and accurate diagnosis and to help identify relevant complications that may have an impact on surgical planning or management.

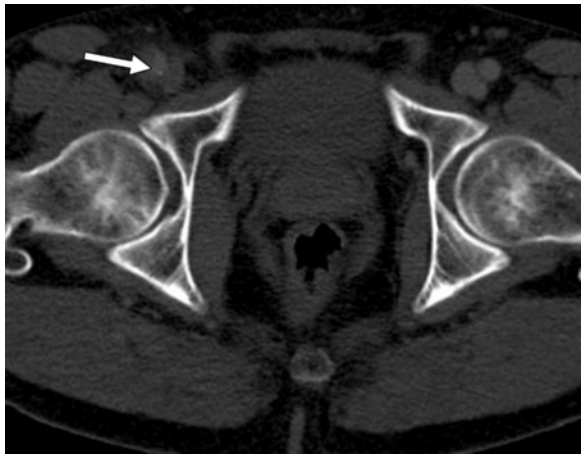

Figure 19. Axial image shows extension of a dissection flap into the right common femoral artery (arrow). This finding emphasizes the need to include the entire aorta and pelvic vessels in the scanning field to detect the full extent of involvement.

References

1. Castañer E, Andreu M, Gallardo X, Mata JM, Cabezuelo MA, Pallardó Y. CT in nontraumatic acute thoracic aortic disease: typical and atypical features and complications. RadioGraphics 2003;23(spec no): S93–S110.
2. Mehta RH, Suzuki T, Hagan PG, et al. Predicting death in patients with acute type a aortic dissection. Circulation 2002;105(2):200–206.
3. Hagan PG, Nienaber CA, Isselbacher EM, et al. The International Registry of Acute Aortic Dissection (IRAD): new insights into an old disease. JAMA 2000;283(7):897–903.
4. Wheat MW Jr. Acute dissecting aneurysms of the aorta: diagnosis and treatment–1979. Am Heart J 1980;99(3):373–387.
5. Nienaber CA, Fattori R, Mehta RH, et al. Gender-related differences in acute aortic dissection. Circulation 2004;109(24):3014–3021.
6. Nienaber CA, Eagle KA. Aortic dissection: new frontiers in diagnosis and management. I. From etiology to diagnostic strategies. Circulation 2003;108 (5):628–635.
7. Svensson LG, Crawford ES. Aortic dissection and aortic aneurysm surgery: clinical observations, experimental investigations, and statistical analyses—II. Curr Probl Surg 1992;29(12):913–1057.
8. Miller DC. The continuing dilemma concerning medical versus surgical management of patients with acute type B dissections. Semin Thorac Cardiovasc Surg 1993;5(1):33–46.
9. Mehta RH, O'Gara PT, Bossone E, et al. Acute type A aortic dissection in the elderly: clinical characteristics, management, and outcomes in the current era. J Am Coll Cardiol 2002;40(4):685–692.
10. Januzzi JL, Isselbacher EM, Fattori R, et al. Characterizing the young patient with aortic dissection: results from the International Registry of Aortic Dissection (IRAD). J Am Coll Cardiol 2004;43(4): 665–669.
11. Suzuki T, Mehta RH, Ince H, et al. Clinical profiles and outcomes of acute type B aortic dissection in the current era: lessons from the International Registry of Aortic Dissection (IRAD). Circulation 2003; 108(suppl 1):II312–II317.
12. Nesser HJ, Eggebrecht H, Baumgart D, et al. Emergency stent-graft placement for impending rupture of the descending thoracic aorta. J Endovasc Ther 2002;9(suppl 2):II72–II78.
13. Slater EE. Aortic dissection: presentation and diagnosis. In: Doroghazi RM, Slater EE, eds. Aortic dissection. New York, NY: McGraw-Hill, 1983; 61–70.
14. DeSanctis RW, Doroghazi RM, Austen WG, Buckley MJ. Aortic dissection. N Engl J Med 1987;317 (17):1060–1067.
15. von Kodolitsch Y, Nienaber CA. Ulcer of the thoracic aorta: diagnosis, therapy and prognosis [in German]. Z Kardiol 1998;87(12):917–927.
16. Stanson AW, Kazmier FJ, Hollier LH, et al. Penetrating atherosclerotic ulcers of the thoracic aorta: natural history and clinicopathologic correlations. Ann Vasc Surg 1986;1(1):15–23.

17. Dähnert W. Cardiovascular disorders: aortic dissection. In: Radiology review manual. 5th ed. Philadelphia, Pa: Lippincott Williams & Wilkins, 2003; 607–609.
18. Williams DM, Lee DY, Hamilton BH, et al. The dissected aorta. III. Anatomy and radiologic diagnosis of branch-vessel compromise. Radiology 1997;203 (1):37–44.
19. Williams DM, LePage MA, Lee DY. The dissected aorta. I. Early anatomic changes in an in vitro model. Radiology 1997;203(1):23–31.
20. Patel PD, Arora RR. Pathophysiology, diagnosis, and management of aortic dissection. Ther Adv Cardiovasc Dis 2008;2(6):439–468.
21. Nicholson T, Patel J. The aorta, including intervention. In: Grainger RG, Allison DJ, Adam A, Dixon AK, eds. Grainger and Allison's diagnostic radiology: a textbook of medical imaging. Vol 1. 5th ed. New York, NY: Churchill Livingstone, 2008; 556–561.
22. Williams DM, Lee DY, Hamilton BH, et al. The dissected aorta: percutaneous treatment of ischemic complications—principles and results. J Vasc Interv Radiol 1997;8(4):605–625.
23. Prêtre R, Von Segesser LK. Aortic dissection. Lancet 1997;349(9063):1461–1464.
24. Daily PO, Trueblood HW, Stinson EB, Wuerflein RD, Shumway NE. Management of acute aortic dissections. Ann Thorac Surg 1970;10(3):237–247.
25. Karmy-Jones R, Aldea G, Boyle EM Jr. The continuing evolution in the management of thoracic aortic dissection. Chest 2000;117(5):1221–1223.
26. Gysi J, Schaffner T, Mohacsi P, Aeschbacher B, Althaus U, Carrel T. Early and late outcome of operated and non-operated acute dissection of the descending aorta. Eur J Cardiothorac Surg 1997;11 (6):1163–1169; discussion 1169–1170.
27. Cambria RP, Brewster DC, Gertler J, et al. Vascular complications associated with spontaneous aortic dissection. J Vasc Surg 1988;7(2):199–209.
28. Abrams HL, Kandarpa K. Dissecting aortic aneurysm. In: Baum S, ed. Abrams' angiography. 4th ed. Philadelphia, Pa: Little, Brown, 1997; 493–520.
29. Kadir S. Arteriography of the thoracic aorta. In: Kadir S, ed. Diagnostic angiography. Philadelphia, Pa: Saunders, 1986; 124–171.
30. Weekly clinicopathological exercises, case 32-1974. N Engl J Med 1974;291(7):350–357.
31. Siegelman SS, Sprayregen S, Strasberg Z, Attai LA, Robinson G. Aortic dissection and the left renal artery. Radiology 1970;95(1):73–78.
32. Larson EW, Edwards WD. Risk factors for aortic dissection: a necropsy study of 161 cases. Am J Cardiol 1984;53(6):849–855.
33. Fisher A, Holroyd BR. Cocaine-associated dissection of the thoracic aorta. J Emerg Med 1992;10(6): 723–727.
34. Miller D. Surgical management of aortic dissections: indications, preoperative management and long-term results. In: Doroghazi RM, Slater EE, eds. Aortic dissection. New York, NY: McGraw-Hill, 1983; 193–243.
35. Appelbaum A, Karp RB, Kirklin JW. Ascending vs descending aortic dissections. Ann Surg 1976;183 (3):296–300.
36. Meredith EL, Masani ND. Echocardiography in the emergency assessment of acute aortic syndromes. Eur J Echocardiogr 2009;10(1):i31–i39.
37. Shiga T, Wajima Z, Apfel CC, Inoue T, Ohe Y. Diagnostic accuracy of transesophageal echocardiography, helical computed tomography, and magnetic resonance imaging for suspected thoracic aortic dissection: systematic review and meta-analysis. Arch Intern Med 2006;166(13):1350–1356.
38. Nienaber CA, von Kodolitsch Y, Nicolas V, et al. The diagnosis of thoracic aortic dissection by noninvasive imaging procedures. N Engl J Med 1993;328 (1):1–9.
39. Börner N, Erbel R, Braun B, Henkel B, Meyer J, Rumpelt J. Diagnosis of aortic dissection by transesophageal echocardiography. Am J Cardiol 1984; 54(8):1157–1158.
40. Erbel R, Alfonso F, Boileau C, et al. Diagnosis and management of aortic dissection. Eur Heart J 2001; 22(18):1642–1681.
41. Willmann JK, Wildermuth S, Pfammatter T, et al. Aortoiliac and renal arteries: prospective intraindividual comparison of contrast-enhanced three-dimensional MR angiography and multidetector–row CT angiography. Radiology 2003;226(3):798–811.
42. Krinsky GA, Rofsky NM, DeCorato DR, et al. Thoracic aorta: comparison of gadolinium-enhanced three-dimensional MR angiography with conventional MR imaging. Radiology 1997;202(1):183–193.
43. Hernández-Hoyos M, Orkisz M, Puech P, Mansard-Desbleds C, Douek P, Magnin IE. Computer-assisted analysis of three-dimensional MR angiograms. RadioGraphics 2002;22(2):421–436.
44. Liu Q, Lu JP, Wang F, Wang L, Tian JM. Three-dimensional contrast-enhanced MR angiography of aortic dissection: a pictorial essay. RadioGraphics 2007;27(5):1311–1321.
45. Prince MR, Narasimham DL, Jacoby WT, et al. Three-dimensional gadolinium-enhanced MR angiography of the thoracic aorta. AJR Am J Roentgenol 1996;166(6):1387–1397.
46. Randoux B, Marro B, Koskas F, et al. Carotid artery stenosis: prospective comparison of CT, three-dimensional gadolinium-enhanced MR, and conventional angiography. Radiology 2001;220(1):179–185.
47. Liu Q, Lu JP, Wang F, Wang L, Tian JM. Endovascular graft exclusion for abdominal aortic aneurysms: 3D contrast-enhanced MR angiography. Abdom Imaging 2006;31(3):347–360.
48. Halpern EJ. Triple-rule-out CT angiography for evaluation of acute chest pain and possible acute coronary syndrome. Radiology 2009;252(2):332–345.
49. Desjardins B, Kazerooni EA. ECG-gated cardiac CT. AJR Am J Roentgenol 2004;182(4):993–1010.

50. Roos JE, Willmann JK, Weishaupt D, Lachat M, Marincek B, Hilfiker PR. Thoracic aorta: motion artifact reduction with retrospective and prospective electrocardiography-assisted multidetector–row CT. Radiology 2002;222(1):271–277.
51. Schoepf UJ, Becker CR, Ohnesorge BM, Yucel EK. CT of coronary artery disease. Radiology 2004;232 (1):18–37.
52. Leung KC, Martin CJ. Effective doses for coronary angiography. Br J Radiol 1996;69(821):426–431.
53. Sebastià C, Pallisa E, Quiroga S, Alvarez-Castells A, Dominguez R, Evangelista A. Aortic dissection: diagnosis and follow-up with helical CT. RadioGraphics 1999;19(1):45–60.
54. Nelsen KM, Spizarny DL, Kastan DJ. Intimointimal intussusception in aortic dissection: CT diagnosis. AJR Am J Roentgenol 1994;162(4):813–814.
55. Karabulut N, Goodman LR, Olinger GN. CT diagnosis of an unusual aortic dissection with intimointimal intussusception: the wind sock sign. J Comput Assist Tomogr 1998;22(5):692–693.
56. Hachiya J, Nitatori T, Yoshino A, Okada M, Furuya Y. CT of calcified chronic aortic dissection simulating atherosclerotic aneurysm. J Comput Assist Tomogr 1993;17(3):374–378.
57. McReynolds RA, Shin MS, Sims RD. Three-channeled aortic dissection. AJR Am J Roentgenol 1978; 130(3):549–552.
58. Williams DM, Joshi A, Dake MD, Deeb GM, Miller DC, Abrams GD. Aortic cobwebs: an anatomic marker identifying the false lumen in aortic dissection—imaging and pathologic correlation. Radiology 1994;190(1):167–174.
59. LePage MA, Quint LE, Sonnad SS, Deeb GM, Williams DM. Aortic dissection: CT features that distinguish true lumen from false lumen. AJR Am J Roentgenol 2001;177(1):207–211.
60. Fisher ER, Stern EJ, Godwin JD 2nd, Otto CM, Johnson JA. Acute aortic dissection: typical and atypical imaging features. RadioGraphics 1994;14 (6):1263–1271; discussion 1271–1274.
61. Rubin GD. Helical CT angiography of the thoracic aorta. J Thorac Imaging 1997;12(2):128–149.
62. Hu H, He HD, Foley WD, Fox SH. Four multidetector-row helical CT: image quality and volume coverage speed. Radiology 2000;215(1):55–62.
63. Dawson P, Lees WR. Multi-slice technology in computed tomography. Clin Radiol 2001;56(4):302–309.
64. Chung JW, Park JH, Im JG, Chung MJ, Han MC, Ahn H. Spiral CT angiography of the thoracic aorta. RadioGraphics 1996;16(4):811–824.

Multidetector CT of Aortic Dissection: A Pictorial Review1

Michelle A. McMahon, FRCR • Christopher A. Squirrell, FRCR

RadioGraphics 2010; **30:445–460** • Published online **10.1148/rg.302095104** • Content Codes: CA CT ER

Page 446
Dissection is the result of a spontaneous longitudinal separation of the aortic intima and adventitia caused by circulating blood gaining access to and splitting the media of the aortic wall (17).

Page 447
Stanford type A dissection involves the ascending thoracic aorta, and the dissection flap may extend into the descending aorta. Type A dissections account for 60%–70% of cases (17) and typically require urgent surgical intervention to prevent extension into the aortic root, pericardium, or coronary arteries (1). If untreated, type A dissections are associated with a mortality rate of over 50% within 48 hours.

Page 447
Stanford type B dissection involves the descending thoracic aorta distal to the left subclavian artery and accounts for 30%–40% of cases (Figs 1b, 3) (17). Management takes the form of medical treatment of hypertension, unless there are complications due to extension of the dissection (eg, end-organ ischemia or persistent pain) that would necessitate surgical intervention.

Page 451
The classic intimal flap is seen in approximately 70% of cases of aortic dissection. It occurs when blood enters the medial layer through an intimal tear, giving rise to a true lumen and a false lumen, with the flap separating the two lumina.

Page 455
In patients with thoracic aortic dissection, death can occur secondary to acute aortic regurgitation, major aortic branch obstruction, pericardial tamponade, or aortic rupture, 75% of which occur into the pericardium, left pleural cavity, or mediastinum.